Transient Current Characteristics of Dispersed Charges in a Non-Polar Medium

Yoocharn Jeon, Pavel Kornilovitch, Patricia Beck, Zhang-Lin Zhou, Richard Henze, Tim Koch

HP Laboratories
HPL-2011-51

Keyword(s):

electrophoretic displays, charge, non-polar medium, transient currents, modeling

Abstract:

Transient currents of reverse micelles in a non-polar solvent from voltage step stimuli were studied to investigate the electrophoretic behavior of the charges. The current showed a sharp peak right after the voltage application and decayed afterward while it exhibited various time-dependent transients depending on the applied voltage and the charge content after the bias was removed. A one-dimensional drift-diffusion model could reproduce the behaviors for various conditions. The forward transient could be well-explained by a simple capacitor charging model with a limited charge. It turned out that the broad peak in the reverse transient current is formed by a competition between an increasing number of charges available for drift and a decreasing electric field resulting from mixing of opposite charges and that the full development of the peak is a good indication of complete polarization of the charges. The slow initial release of charges from the electrodes is due to the electric field developed by accumulated charges that decreases as the charges are released by diffusion. The high density compaction of charges against the electrodes reduces electric field screening by the accumulated charges and enables more accumulation, but individual charge-to-charge interaction limits the density.

External Posting Date: April 21, 2011 [Fulltext] Approved for External Publication
Internal Posting Date: April 21, 2011 [Fulltext]

Transient Current Characteristics of Dispersed Charges in a Non-Polar Medium

Yoocharn Jeon, Pavel Kornilovitch*, Patricia Beck, Zhang-Lin Zhou, Richard Henze, and Tim Koch*

Hewlett-Packard Co., HP Labs, 1501 Page Mill Road, Palo Alto, CA, 94304, USA

* Hewlett-Packard Co., IPG, 1000 NE Circle Blvd. Corvallis, OR, 97330, USA

ABSTRACT

Transient currents of reverse micelles in a non-polar solvent from voltage step stimuli were studied to investigate the electrophoretic behavior of the charges. The current showed a sharp peak right after the voltage application and decayed afterward while it exhibited various time-dependent transients depending on the applied voltage and the charge content after the bias was removed. A one-dimensional drift-diffusion model could reproduce the behaviors for various conditions. The forward transient could be well-explained by a simple capacitor charging model with a limited charge. It turned out that the broad peak in the reverse transient current is formed by a competition between an increasing number of charges available for drift and a decreasing electric field resulting from mixing of opposite charges and that the full development of the peak is a good indication of complete polarization of the charges. The slow initial release of charges from the electrodes is due to the electric field developed by accumulated charges that decreases as the charges are released by diffusion. The high density compaction of charges against the electrodes reduces electric field screening by the accumulated charges and enables more accumulation, but individual charge-to-charge interaction limits the density.

Keywords: electrophoretic displays, charge, non-polar medium, transient currents, modeling

1. INTRODUCTION

Electrophoretic control of charged particles has been used for reflective displays and is getting increasing attention. Since charge motion results in an electric current, the transient current is a useful tool to understand how the charges move in the display cell. A simple initial gradual decay and a broad reversal peak were observed in transient currents of Aerosol OT solution in xylene and interpreted as a result of transition of charges in conjunction with dissociation and recombination of ionic species. [1-2] Similar behaviors were observed in OLOA1200 solutions in non-polar solvents, [3-5] Electric field shielding by accumulated charges and delay time with a normal distribution were used to explain the origin of the broad peak in the reversal currents, respectively. [3-4] However, these previous efforts to interpret the transient current behaviors were abstract and have not resulted in a thorough understanding of all the phenomena. In this article we give a clear and thorough explanation of the origin of the reserve transient current peak by presenting transient current measurement data of non-polar solutions for various voltages and surfactant concentrations and comparing them with numerical simulations of a one-dimensional model.

2. EXPERIMENTS

Dispersions of poly-isobutylene succinimide (OLOA11000, Chevron) in an iso-paraffinic solvent in various concentrations were used as model electrophoretic fluids. The dispersions were placed in parallel-plate electrodes with an area of 0.5 cm^2 separated by 10 microns without any insulation on them. A voltage step of 0.1 – 10 volts was applied across the solution and the forward transient current was measured for 5 seconds, during which the current subsided to zero. The reverse transient current was measured for another 5 seconds after the applied voltage was brought down to zero volts. The test cells used had a parallel-plates geometry. The current through the test cells was measured after application and removal of a voltage step of various magnitudes.

3. NUMERICAL MODELING

A one-dimensional model has been built and solved numerically using COMSOL Multiphysics. The charge flux is a sum of the drift and diffusion contributions. The concentration of a charge species c_i (c_+ or c_-) satisfies the local mass conservation equation,

$$\partial c_i / \partial t + \nabla \cdot \left(- D_i \nabla c_i - (\mu_i \nabla \phi) c_i \right) = 0 , \qquad (1)$$

where D_i is the diffusion coefficient, μ_i the electrophoretic mobility, and ϕ the electrostatic potential. The

electrostatic potential is governed by the Poisson equation,

$$-\varepsilon_0\varepsilon_r \nabla\cdot\nabla\phi = q(c_+ - c_-)\,, \tag{2}$$

where ε_0 is the dielectric constant of vacuum, ε_r the relative dielectric constant of the solution, and q the elementary charge. Blocking boundary condition was used assuming no Faradaic reaction on the electrodes. The current was calculated using

$$J = \varepsilon_0\varepsilon_r \left.\frac{\partial\nabla\phi}{\partial t}\right|_{x=0}\,. \tag{3}$$

It is also assumed that the mobilities of the positive and the negative charges are identical and that each charge has one elementary charge only. When individual charge-to-charge interactions were considered, linear elastic compression is assumed for charges closer than 50 nm to one another by multiplying D_i. by $(1+k(d_p - d_{po}))$, where k is a modified elastic constant, d_p intercharge distance calculated from the local charge concentration, and d_{po} maximum interaction distance (50 nm). The initial conditions are $\phi = 0$ and $c_+ = c_- = c_0$ for all positions. All the parameters used in the modeling were directly extracted from the corresponding experimental data except for k and d_{po} which cannot be directly measured.

4. RESULTS AND DISCUSSION

Fig.1 shows transient currents from 3 wt% OLOA11000 dispersion for various voltages. After the voltage is applied, the current shows a sharp peak and then gradually decreases to zero. After the voltage is brought down to zero volts at 5 seconds, the reverse transient current that follows shows different behaviors from the forward transient depending on the magnitude of the step voltage.

4.1 Forward Transient Currents

The detailed behaviors of the forward transient currents were shown in Fig.2. The initial peak current is proportional to the applied voltage for the whole range of the voltage used. For the voltages lower than 1 V the current decreases exponentially with time after a short faster decay in the beginning. This can be modeled as capacitor(C_{int}) charging with a series resistance(R_0). At the early stage of the transition all charges in the cell are moved by the applied electric field, which produces a high peak current with a magnitude proportional to the voltage. The charges moved by the applied electric field are accumulated at the electrode interfaces. The charge accumulation (Q_{acc}) at the interfaces can be represented by a capacitor (C_{int}) and charging the capacitor builds up a potential ($V_{int} = Q_{acc}/C_{int}$), which reduces the effective electric field in the middle of the cell that drives the charges ($E_{eff} = (V_{app} - V_{int})/d_{cell}$). When the accumulated charge is small compared to the total charge

content in the cell, the bulk conductivity can be assumed constant and the current can be easily calculated as $I(t) = I_0\exp(-t/\tau)$, where $\tau = R_0C_{int}$. [2] This simple model predicts that the current should exhibit a same slope for different voltages. However, the experimental data show that the current decays more slowly for higher voltages up to 0.75 V and it decreases increasingly faster as the voltage increases higher than 1 V. The same deviation from the simply exponential decay has been reported and the attempt to explain it by varying capacitance by double layer thickness change was not fully successful. [6] This deviation can be better explained even with fixed a capacitance by taking it into account that only the charges remaining in the cell are available to be moved by the electric field while the charges that have reached an electrode cannot move any further. When the bulk resistance is adjusted as $R = R_0(1 - Q_{acc}/Q_{total})$, the transient current can be expressed in a general form of

$$I(t) = I_0(1-\beta)^2 \frac{e^{(1-\beta)t/\tau}}{\left(e^{(1-\beta)t/\tau} - \beta\right)^2}, \quad (4)$$

where the constant $\beta = C_{int}V_{app}/Q_{total}$ is the ratio of maximum charge that can be stored in the interface capacitors at the given voltage to the total charge in the system. The transient currents from the capacitor charging model with adjusted bulk resistance are shown in Fig.3, which fits the experimental results very well for the whole range of voltage and time. As the voltage increases from 0.25 V to 1 V ($\beta < 1$), the current decay gets slower at higher voltages because the less charges are remaining in the middle of the cell to be transported and accumulated in the capacitors in the later stage while the electric field screening by the accumulated charges is the cause that slows down the transport. The current decreases to zero when the space charge completely screens the applied field. However, as the voltage increases further higher than 1 V, enough to compact all the charges against the electrodes ($\beta > 1$), the transition ends when all the existing charges are swept away to the electrodes since the electric field is not completely screened by the accumulated charges even when the all charges are collected at the electrodes. Once all the charges are collected at the electrodes, the effective field lowering is constant and the sweeping of the charges gets faster at higher voltages. As a result the current decreases more quickly at a higher voltage. When the applied voltage is much higher than the potential buildup at the interface capacitors ($V_{app} >> V_{int} = Q_{acc}/C_{int}$, $\beta >> 1$), the screening from the charge accumulation is not significant and the current decreases linearly with time with a slope proportional to the applied voltage.

The transient current behaviors have been reproduced more accurately by a one-dimensional numerical

drift-diffusion model as shown in Fig.4. In this model the local distributions of the charges and the electric field were considered while they were assumed constant throughout the cell in the capacitor charging model with limited charges. Even though the more sophisticated model fits the experimental data more accurately, most of the behaviors can be explained well with the simple capacitor charging model with limited charges. It means that the effective field lowering by the interface capacitor charging and the decrease in movable charges are the main factors governing the forward transient while the local distribution of the charges and the electric field play minor roles, which was pointed out as a major factor in [5].

4.2 Reverse Transient Currents

Fig.5 shows the measured reverse transient currents of 3 wt% OLOA11000 dispersion after various voltage biases of 5 seconds were removed. When the voltage is lower than 0.5 V, the reverse current decays monotonically in a similar way to the forward current. At step voltages higher than 0.5 V the reverse current develops a broad peak. The peak shifts to later times as the voltage increases up to 1 V. After that, the shape and the position of the peak do not change significantly. The simple capacitor discharging model cannot explain the development of the broad peak because the model predicts a simple exponential decay. In the model all the accumulated charges should be available for the reverse transit from the beginning of the reverse transient and only the driving electric field should decay as the charges are released from the capacitors.

All important features in the transient current of the experiments have been reproduced by the drift-diffusion model, including the delayed broad peak as shown in Fig.6. This model shows the charge and electric field distributions are quite symmetric, but the diffusion fluxes are antisymmetric about the center of the cell except for narrow regions next to the electrodes. Spatial integration of the diffusion fluxes, which is their net contribution to the external current, is insignificant in comparison with their drift counterparts because of the anitisymmetry. Therefore the transient current is mainly governed by the drift fluxes. Since the drift flux is a product of the charge concentration and the local electric field, the current behavior can be explained by observing how they change over time. Fig.7 shows the drift flux at the center of the cell, which is the product of the local electric field and the charge concentration. This agrees closely with the external current. In the early stage of the reversal the increase in current is mainly driven by the increase in the charge concentration rather than by the change in the local electric field. At equilibrium under bias, the diffusion and drift fluxes completely balance each other throughout the length of the cell. When the applied voltage is removed (at $t = 5$ s), the balance between the drift and diffusion is broken, which gives rise to a reverse current. The driving force for the

drift is the electric field generated by the accumulated charges. At the early stages of the reversal the current from the charges moving away from the electrodes is small because most of the charges are still held near the electrodes where they are being pushed against the electrodes by local electric fields generated by the spatial distribution of the charges, as shown in Fig.8 (t = 5.01 s). Because the diffusion flux is larger than the drift, the charges diffuse toward the cell center where they are more susceptible to the local electric field that pushes them toward the opposite electrodes (t = 5.43 s). As the charges move away from the electrodes, the opposite charge induced in the electrode by the charge in the cell decreases. It reduces the electric field that holds the charges in the cell near the electrodes against the diffusion and allows faster release of the charges into the region where the electric field drives them toward the opposite electrodes. As a result the current increases exponentially with time in the early stage. In the later stage (t > 5.43 s) as charges of two opposite polarities mix in the bulk of the cell, the space charge, which is the main driving force of the reverse transient, diminishes with time. The charge distribution becomes more even throughout the cell, which also reduces the diffusion fluxes. The current decreases because the electric field decreases faster than the charge concentration increases.

When the applied voltage is not large enough to polarize the entire population of charged species ($\beta < 1$), a significant amount of charge is left in the middle of the cell. As a result, it can contribute to the electrophoretic drift from the beginning of the reversal, which produces a high initial reverse current.(V = 0.25 - 0.5 V in Fig.5 and Fig.6) As the polarization becomes more complete with increasing bias, less charge is available for the initial drift and it takes longer to reach the peak current.(V = 0.75 - 1 V in Fig.5 and Fig.6) However, once the voltage reaches the value that is sufficient to polarize the entire charge in the system (V > 1 V or $\beta > 1$ in capacitor charge model with limited charge), no further increase in the bias will change the charge distribution in the cell. The reverse current response stops changing because the entire process is determined by the initial charge distribution profile.(V = 1.25 - 2 V in Fig.5 and Fig.6, $\beta > 1$) Therefore, the degree of the reverse peak development is a good measure of the completeness of polarization.

Individual charge interaction plays an important role in charge compaction at the electrodes. Though the model describes the overall behaviors very well, it deviates from the experimental data at high charge concentrations if the charge-to-charge interaction is ignored. As seen in Fig.9(c) and Fig.10(c), the model without inter-charge interaction predicts that the reverse peaks appear later than the experiments. This is because the model assumes point charges, which permits unrealistically high local charge concentrations in the vicinity of the electrodes. This makes it underestimate the electric field buildup and predict complete

polarization at a lower voltage than reality. And the lower electric field estimation from the space charge slows down the rise of the reverse drift, which ends up with the shift of the peak position to a later time. This error gets worse as the charge content increases as in Fig.9. The model with point-charge assumption predicts later appearance of the peak as the total charge content increases while the experimental data shows that the peak stops shifting as the charge concentration increases higher than 1.3×10^{-5} C/cm^3. However, when linear elastic compression is assumed when the charges are compacted closer than 50nm to one another (Fig.9(a) and Fig.10(a)), the model fits the experimental results (Fig.9(b) and Fig.10(b)) very closely. The charge concentrations used in the model was determined from experimental data according to the method described below and the electrophoretic mobility was calculated from the conductivity from the initial forward transient current using the charge concentration.

Under complete polarization, the time integral of the forward or reverse transient current is equal to a half of the total charge content (V > 1 V, $\beta > 1$) while it is a half of the charge that the applied voltage can store in an interface capacitors when the polarization is incomplete (V < 1 V, $\beta < 1$). The charge concentration-equivalent current integrals are shown in Fig.11. The values coincide well with one another for both forward and reverse transients, and also for experiments and model. The current integrals increase superlinearly with the applied voltage when V < 1 V, which means decreasing capacitance [6], while it flats out when V > 1 V. Therefore, one can easily estimate the charge content by integrating the experimental data under a sufficiently large voltage. The experimental data of the 3 wt% OLOA11000 dispersion showed the exact same trend as predicted by the model, and the single polarity charge concentration of 4.6×10^{-5} C/cm^3 is obtained from the measured data and used for numerical and analytical models. Using the conductivity of 4.6×10^{-10} S/cm obtained from the initial forward currents, which is in agreement with impedance spectra measurements, the mobility of the charge carriers is estimated as 1.0×10^{-5} cm^2/Vs. A good agreement between the model and the experimental results confirms the absence of any significant charge generation or charge injection in the system, as assumed in the model.

5. SUMMARY

Step-voltage transient current responses of surfactant dispersions have been measured and analyzed. At step voltages above a certain value, the reverse current shows a broad hump after voltage is removed while the forward current shows a simple decay with a voltage-dependent slope. The behavior could be accurately reproduced by a one-dimensional drift-diffusion model. The forward transient could be also modeled as

capacitor charging with limited charge content. The numerical analysis revealed that the reverse current hump appears as a result of competing contributions of an increasing number of charges available for drift and a decreasing electric field resulting from mixing of opposite charges. Charge-to-charge interaction plays a important role in limiting charge accumulation density and should be taken into account to accurately describe high charge content systems. From the measurement data the total charge content and the electrophoretic mobility has been determined.

REFERENCES

[1] V. Novotny and M. A. Hopper, “Transient Conduction of Weakly Dissociating Species in Dielectric Fluids” *J. Electrochem. Soc*., **126**, No.6. 925-929 (1979)

[2] V. Novotny, “Electrical Conduction in Surfactant-Water-Nonaquous Liquid Systems” *J. Electrochem. Soc*., **133**, No.8. 1629-1636 (1986)

[3] T. Bert, F. Beunis, H. De Smet, K. Neyts, “Transient Current Properties in Electronic Paper” *Proc. IDW*, 1749-1752 (2004)

[4] T. Bert, H. De Smet, F. Beunis, and F. Strubbe, “Numerical simulation of the transport of particles in electrophoretic displays” *Opto-electronics Rev*., **13**, No.4. 281-286 (2005)

[5] F. Beunis, F. Strubbe, K. Neyts, T. Bert, H. De Smet, A. Verschueren, and L. Schlangen, “Electric Field Compensation in Electrophoretic Ink Displays,” *Proc. IDRC*, 344-345 (2005)

[6] J. Kim, J. Anderson, S. Garoff, and L. Schlangen, “Ionic Conduction and Electrode Polarization in a Doped Nonpolar Liquid" *Langmuir*, **21**, No. 19, , 8620-8629 (2005)

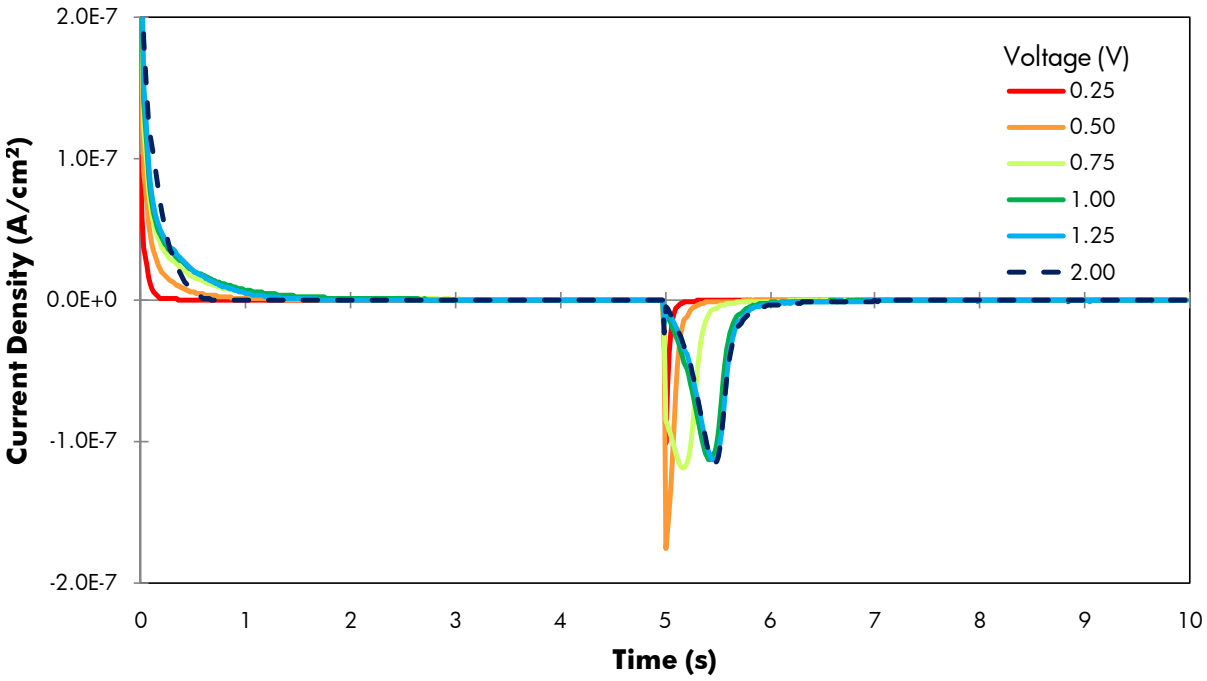

Fig. 1 Transient current responses measured from 3 wt% OLOA11000 dispersion

The currents were measured with parallel-plates electrodes. The distance between the electrodes was 1×10^{-3} cm.

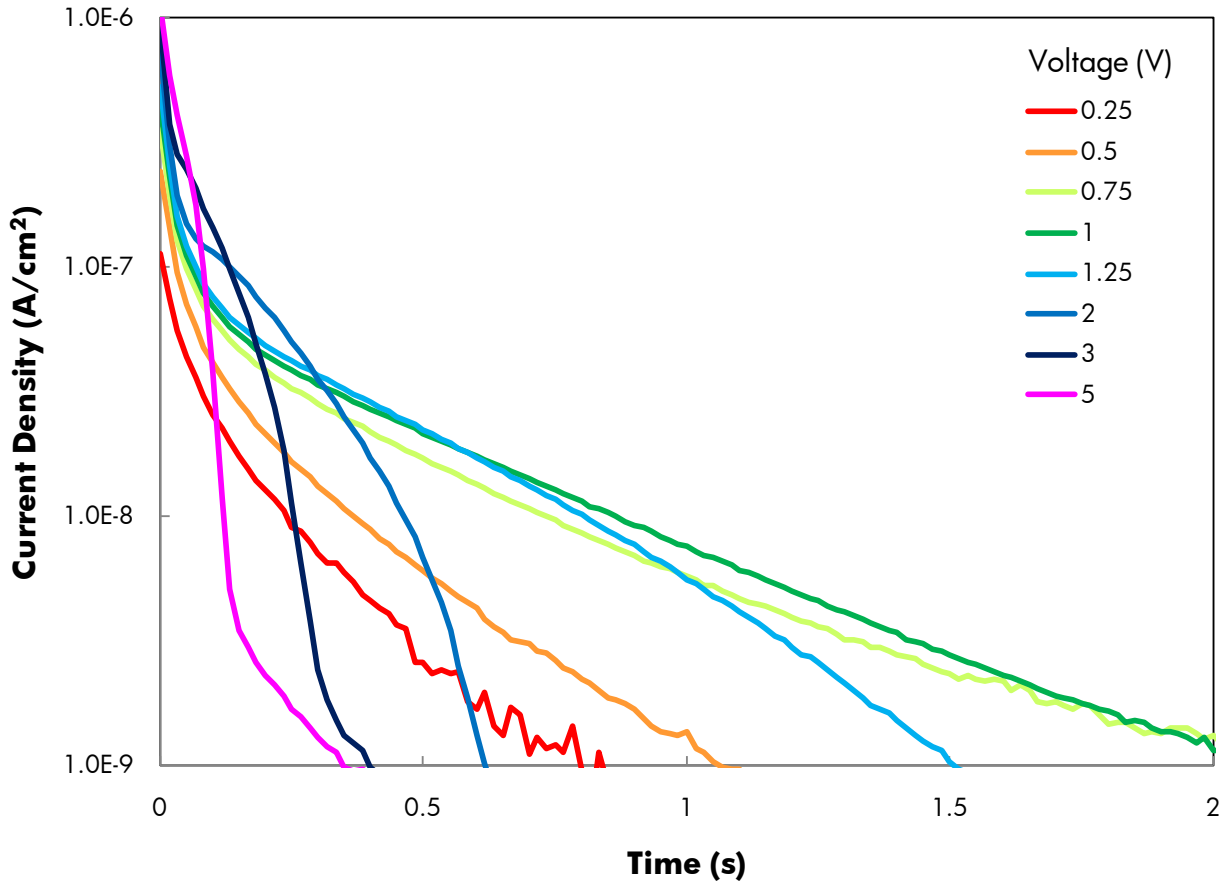

Fig.2 Forward transient currents measured from 3wt% OLOA11000 dispersion

The currents were measured with parallel-plates electrodes. The distance between the electrodes was 1×10^{-3} cm.

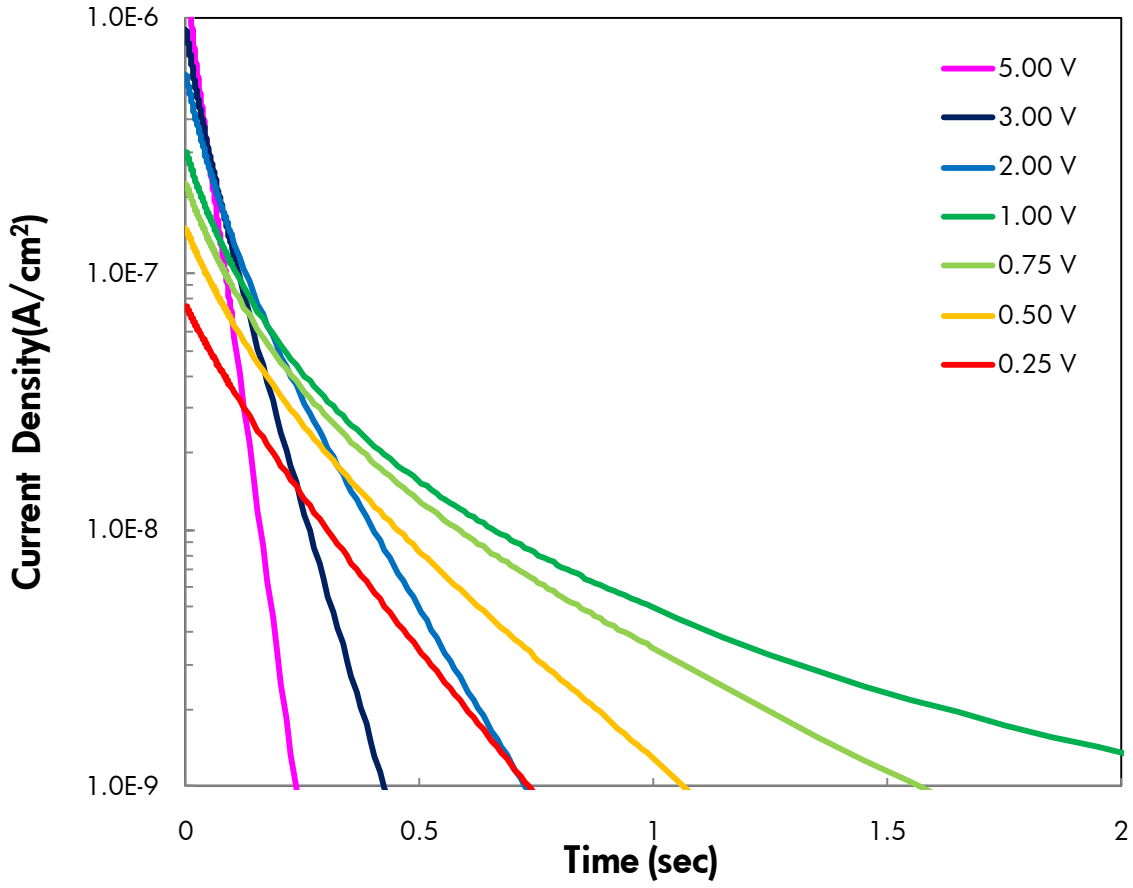

Fig.3 Forward transient current calculated from capacitor charging model with limited charge content Parameters used: $R_0 = 3.3\times10^6\ \Omega\text{cm}^2$, $C_{int} = 4.5\times10^{-8}\ \text{F/cm}^2$, $Q_{total} = 4.5\times10^{-8}\ \text{C/cm}^2$

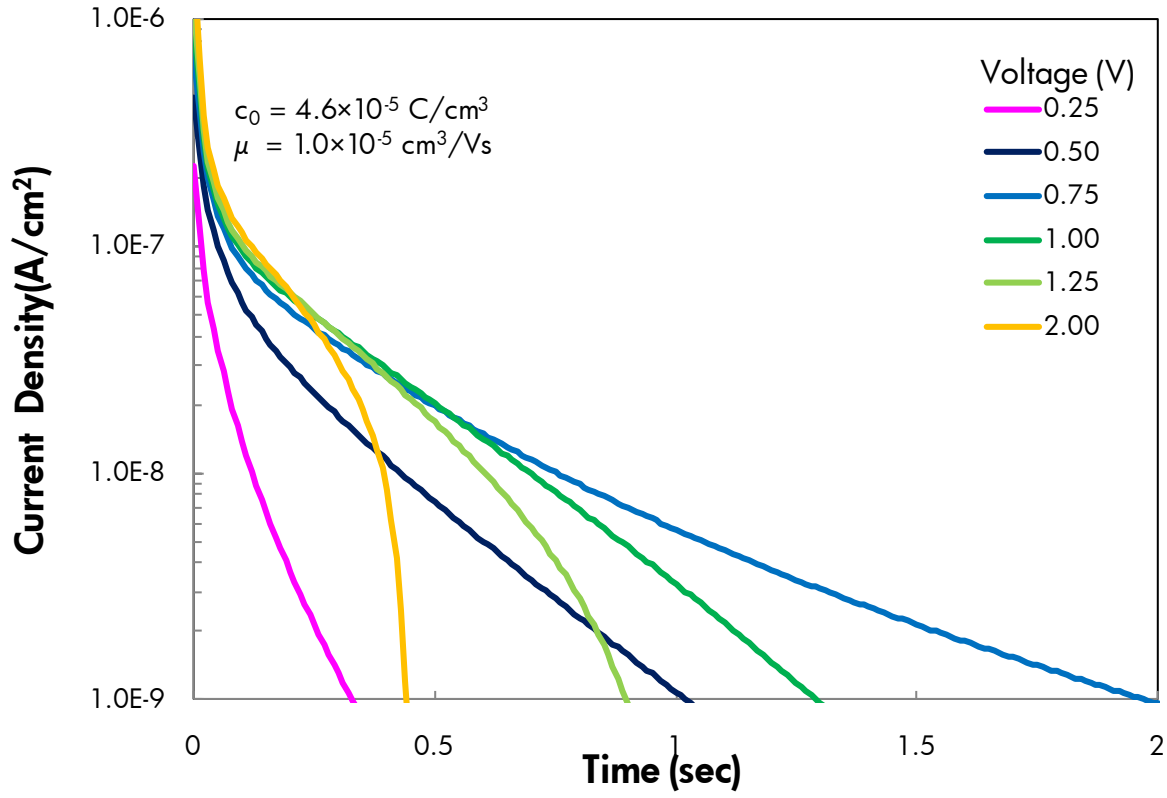

Fig.4 Forward currents calculated from 1-D drift-diffusion numerical model Parameters used: total charge concentration 4.6×10^{-5} C/cm^3, charge mobility 1×10^{-5} cm^2/Vs, electrode spacing 1×10^{-3} cm, elastic particle interactions when closer than 50nm

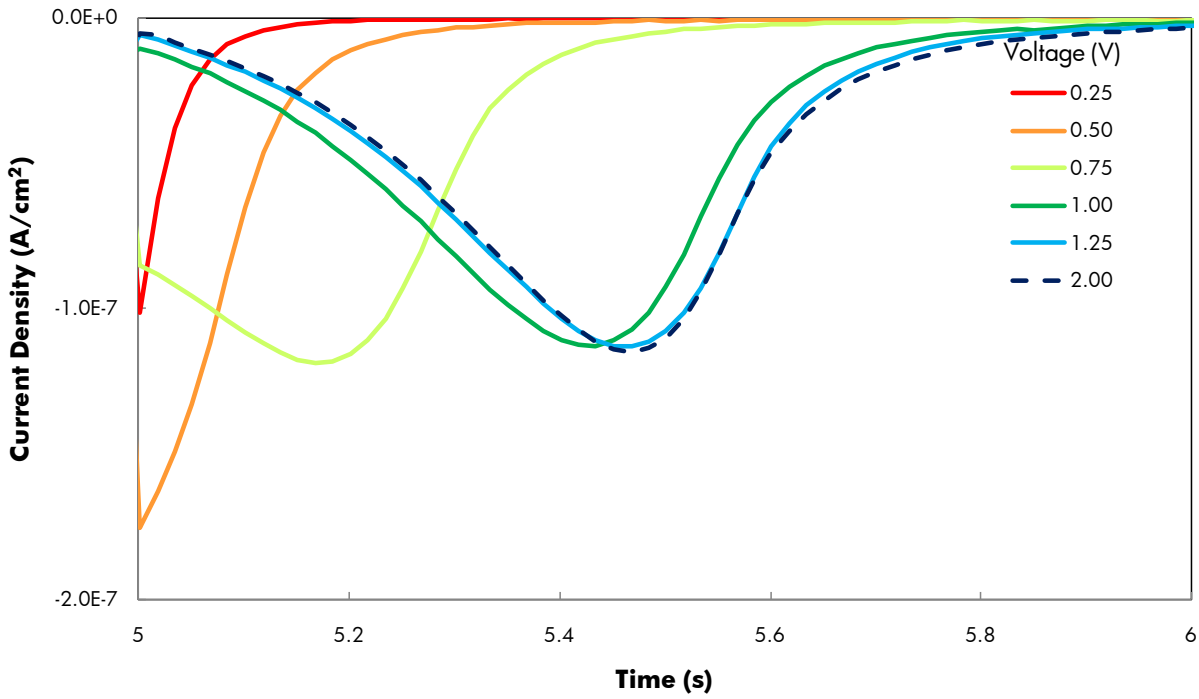

Fig.5 Reverse transient currents measured from 3wt% OLOA11000 dispersion

The currents were measured with parallel-plates electrodes. The distance between the electrodes was 1×10^{-3} cm. The applied voltage is removed at 5 s.

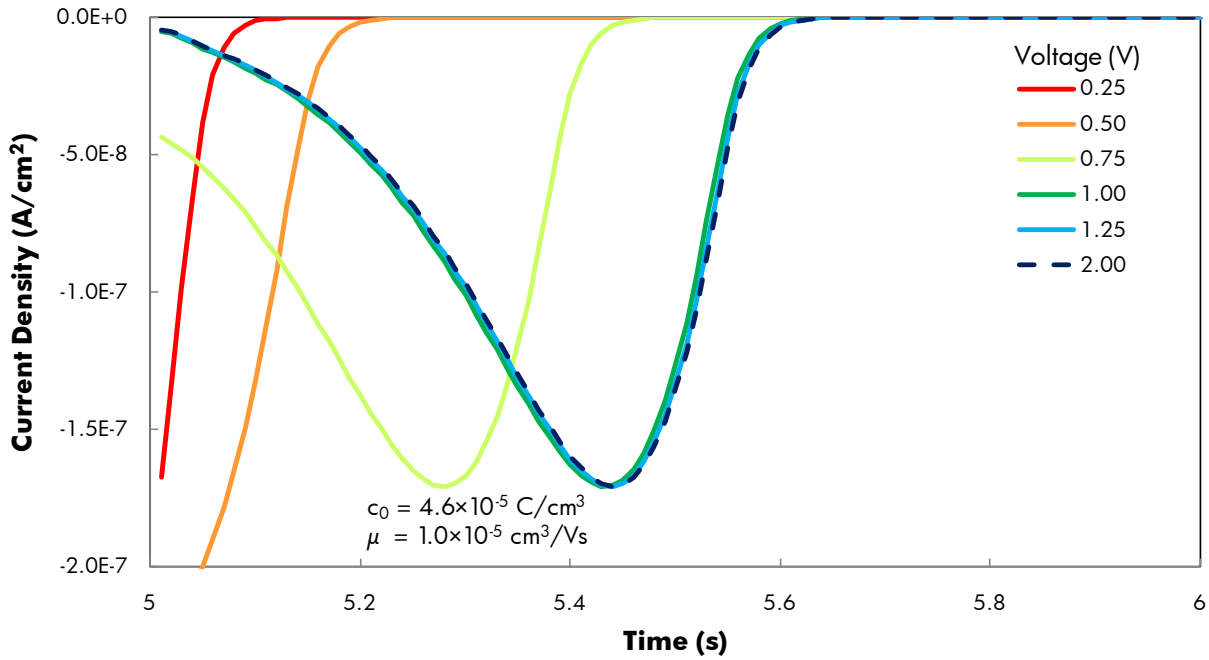

Fig.6 Reverse transient currents calculated from 1-D drift-diffusion model Parameters used: total charge concentration 4.6×10^{-5} C/cm^3, charge mobility 1×10^{-5} cm^2/Vs, electrode spacing 1×10^{-3} cm, elastic particle interactions when closer than 50nm. The applied voltage is removed at 5 s.

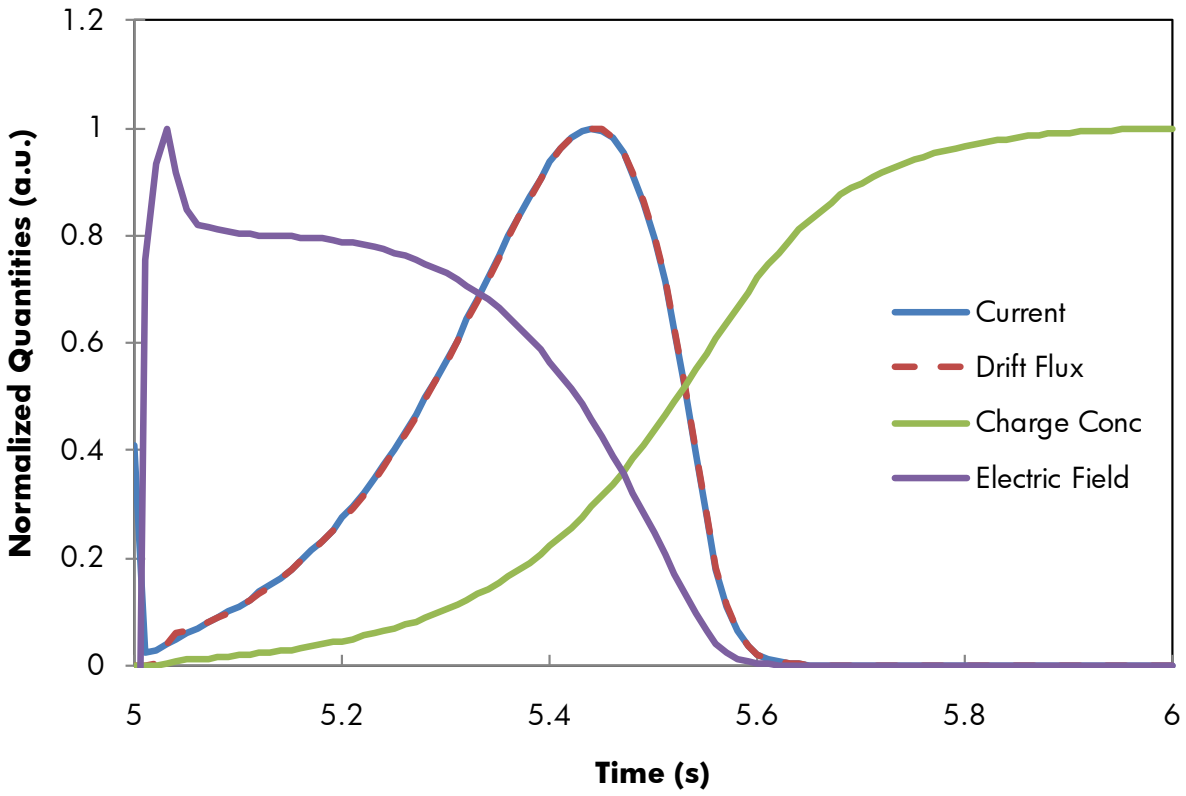

Fig. 7 Two major contributions to reverse transient current behavior The reverse transient current is compared with the drift flux at the center of the cell. 2 V is removed at 5 s.

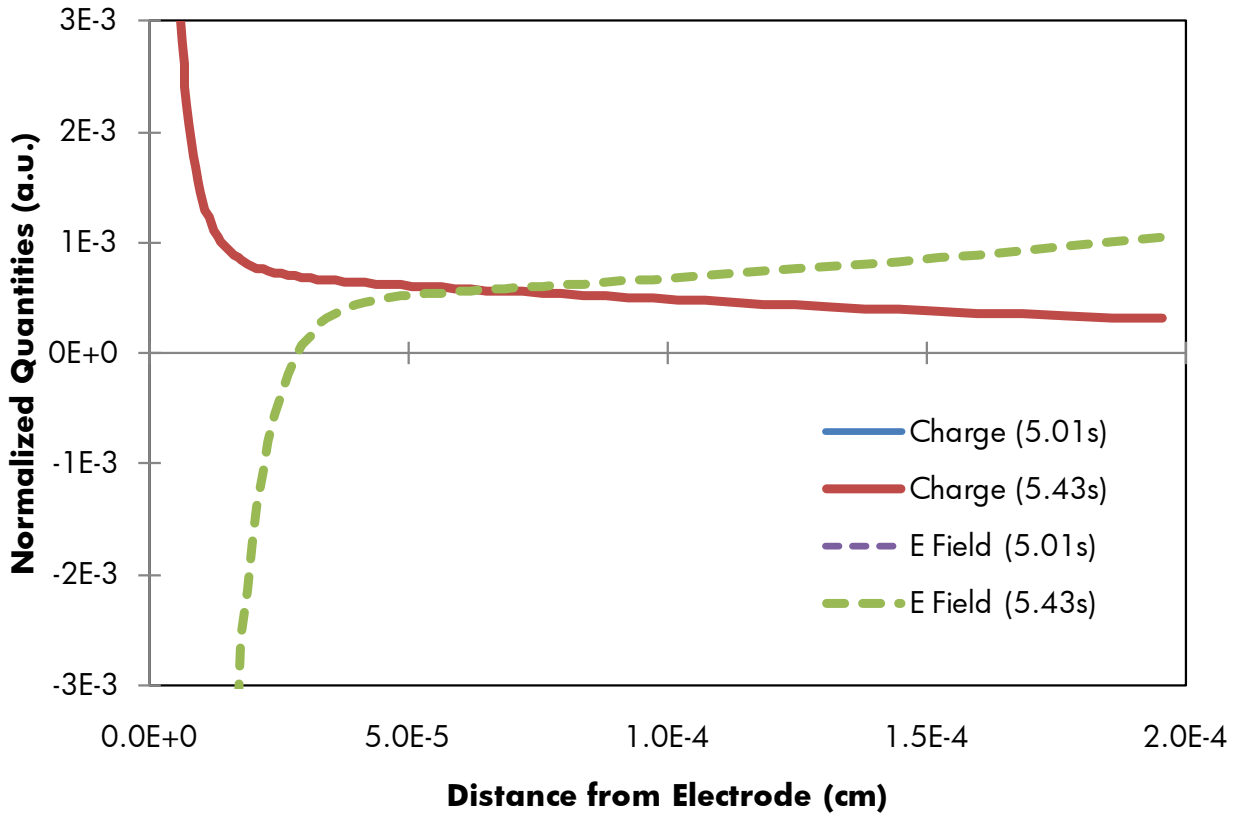

Fig. 8 Normalized positive charge concentration and electric field near an electrode

Parameters used: total charge concentration 4.6×10^{-5} C/cm^3, charge mobility 1×10^{-5} cm^2/Vs, electrode spacing 1×10^{-3} cm, elastic particle interactions when closer than 50nm. The applied voltage of 2 V is removed at 5 s.

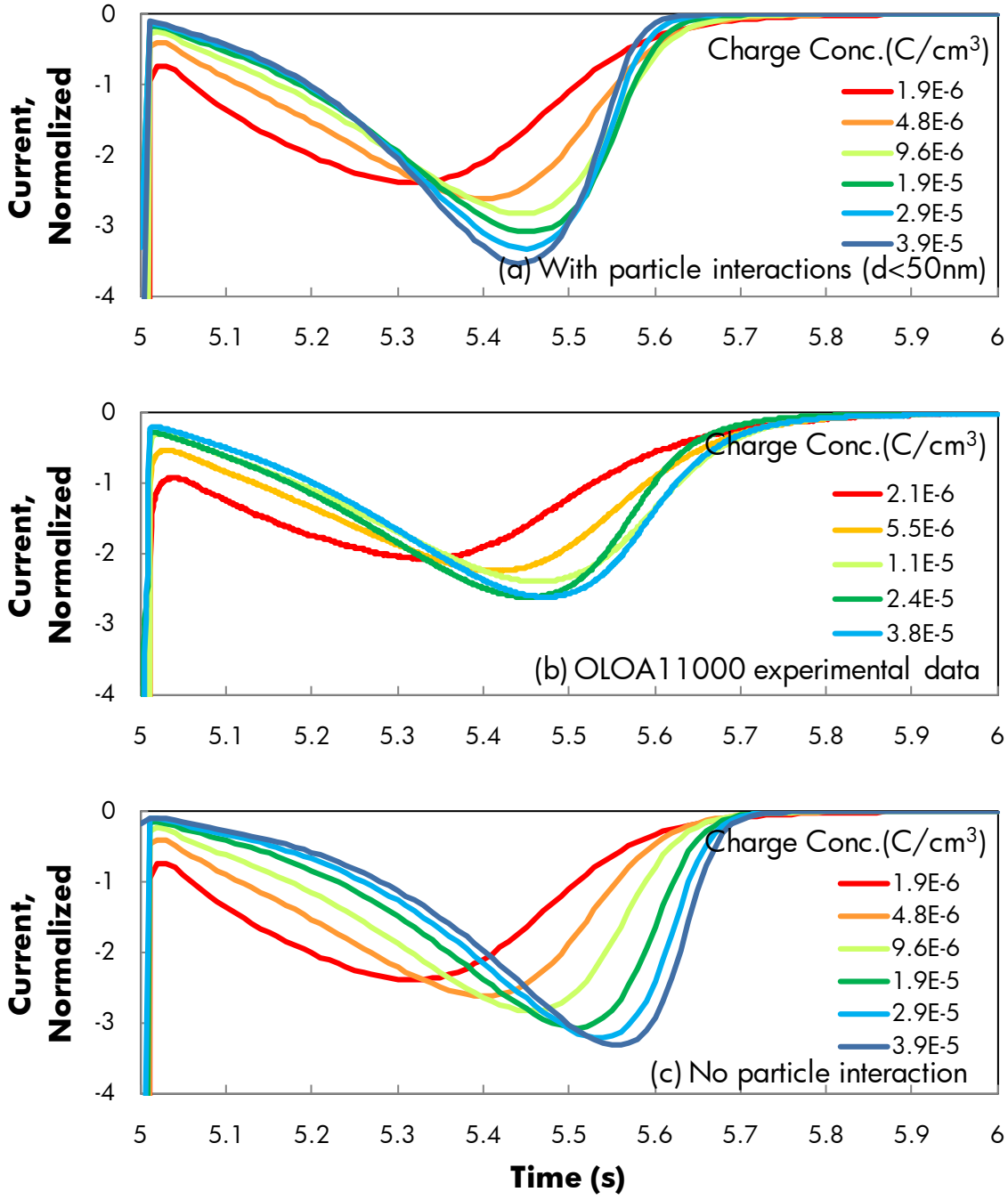

Fig. 9 Reverse transient currents from experiments and models for various charge concentrations
Parameters used: applied voltage 2 V, charge mobility 1×10^{-5} cm^2/Vs, electrode spacing 1×10^{-3} cm. The applied voltage is removed at 5 s.

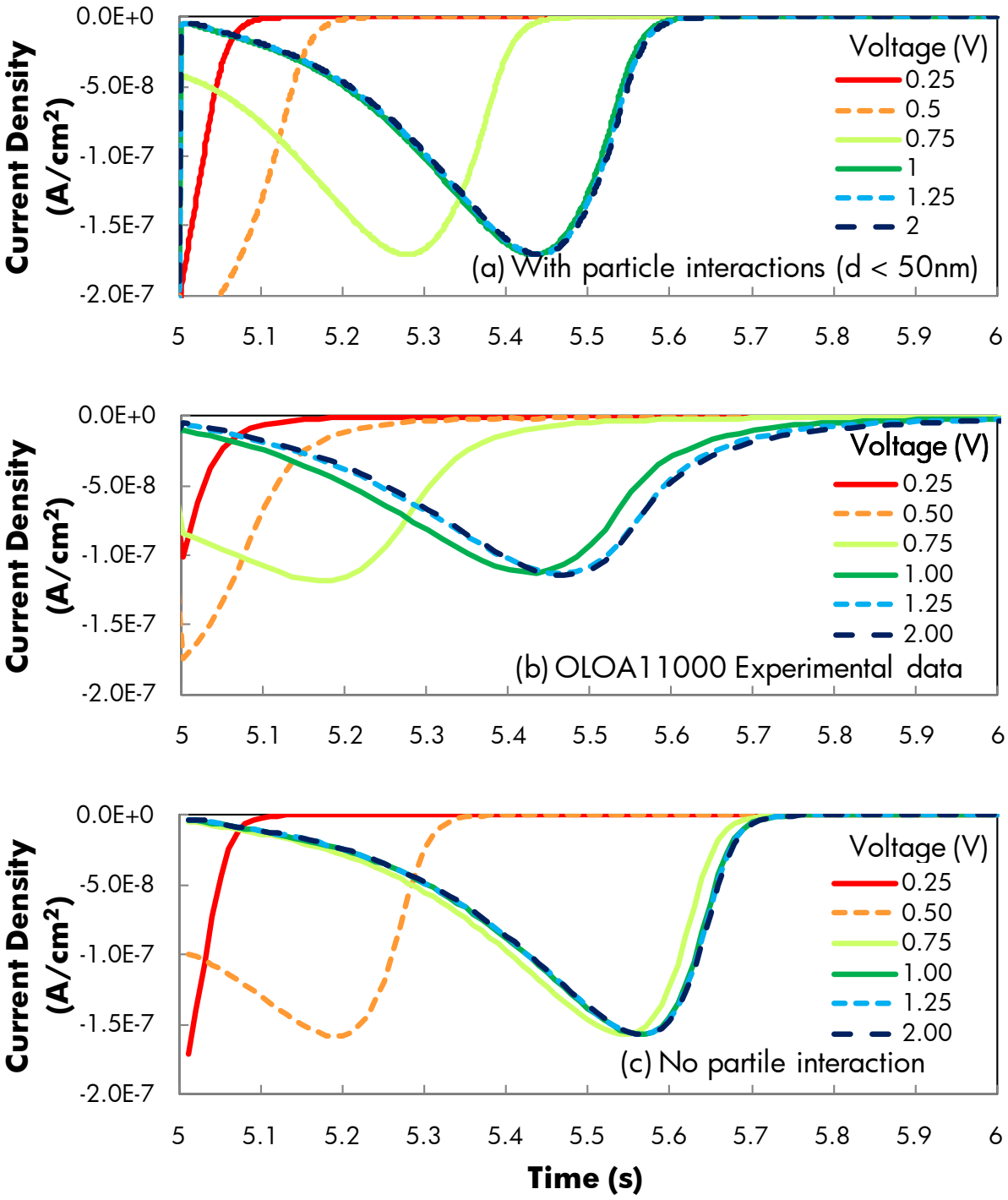

Fig.10 Reverse transient currents from experiments and models for various applied voltages Parameters used: total charge concentration 4.6×10^{-5} C/cm^3, charge mobility 1×10^{-5} cm^2/Vs, electrode spacing 1×10^{-3} cm. The applied voltage is removed at 5 s.

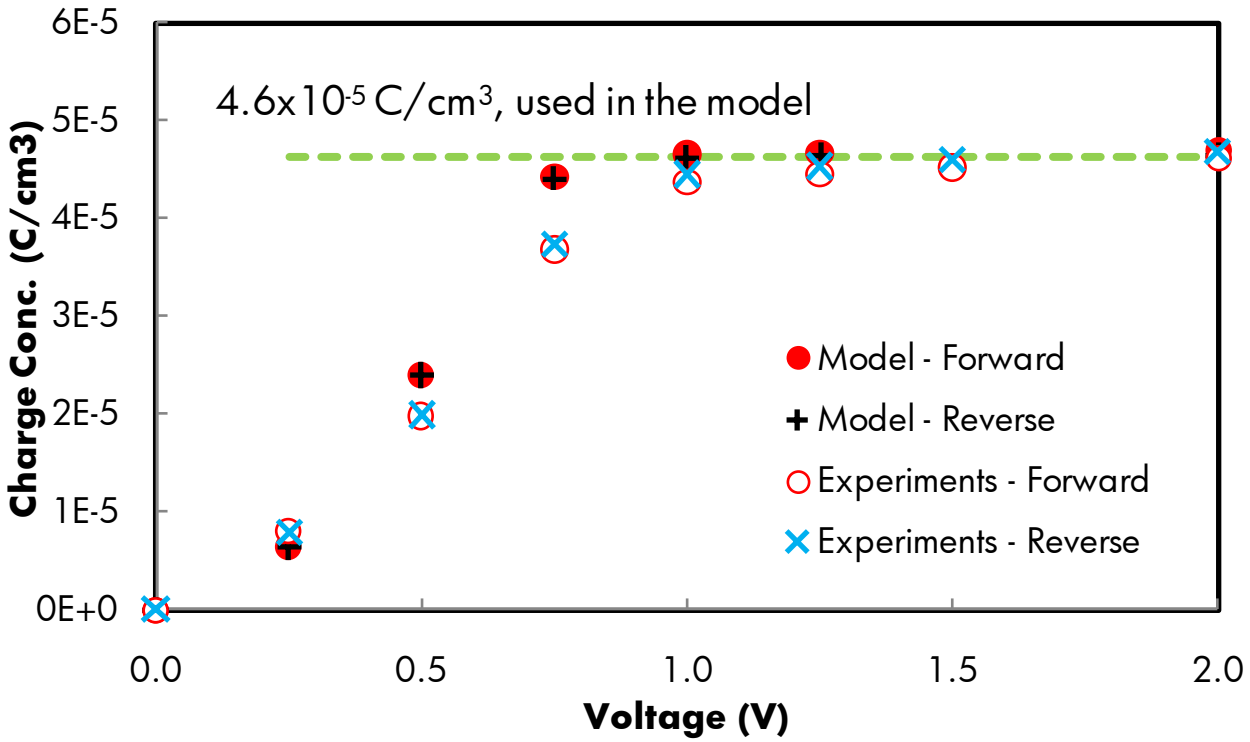

Fig.11 Charge concentrations from transient current integral of 1-D model and experiments

Parameters used: total charge concentration 4.6×10^{-5} C/cm^3, charge mobility 1×10^{-5} cm^2/Vs, electrode spacing 1×10^{-3} cm, elastic particle interactions when closer than 50nm. Experimental data are from 3 wt% OLOA11000 dispersion.